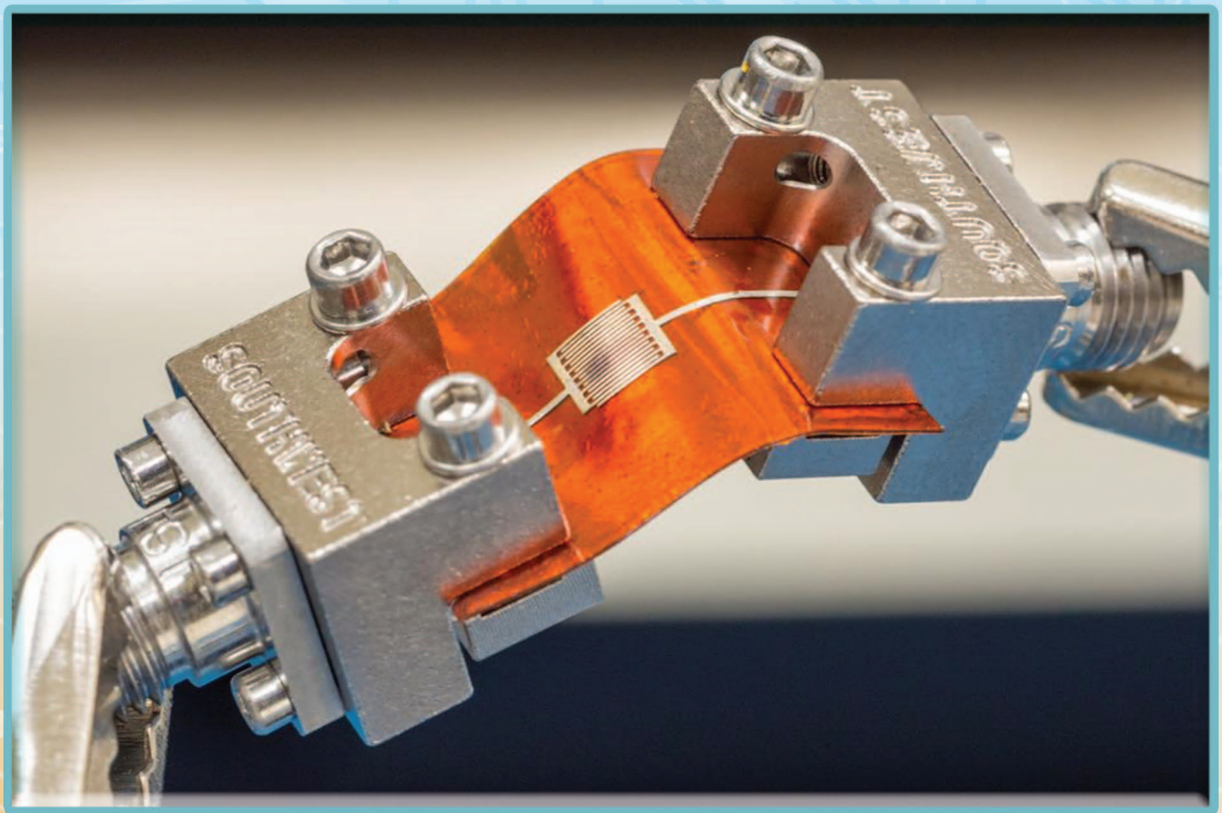

Nanotechnology-Empowered Flexible Printed Wireless Electronics

A review of various applications of printed materials.

ALINE EID, JIMMY HESTER, YUNNAN FANG, BIJAN TEHRANI,
SYED ABDULLAH NAUROZE, RYAN BAHR, AND MANOS M. TENTZERIS

Digital Object Identifier 10.1109/MNANO.2018.2869233
Date of publication: 14 December 2018

 1932-4510/19©2019IEEE

IN THIS ARTICLE, THE PARTICULAR importance of nanotechnology-enabled materials associated with additive manufacturing techniques for the realization of radio-frequency (RF) components and modules for Internet of Things (IoT) and millimeter-wave (mm-wave) applications is discussed. First, a look into the preparation of functional nanomaterial inks for chemical sensing applications and the surface modification processes required for their excellent printability is provided. The focus then shifts toward numerous applications realized through the implementation of the previously listed techniques. These applications discuss origami [morphing/four-dimensional (4D)-printed] structures, taking advantage of the unique benefits of bending and folding on the printed conductive nanomaterials-based traces on a paper substrate for the fabrication of foldable reconfigurable RF architectures. Then, the synergistic integration of inkjet-printed carbon-based nanomaterials sensors with ultrahigh performance flexible printed antenna structures—utilizing nanoparticles—for the Internet of Skins, smart cities, and 5G applications is described. We then demonstrate the critical importance of nanomaterial-based inks in the development of robust three-dimensional (3D)-printed RF interconnects with groundbreaking performance, opening the door for the next generation of electronics manufacturing and packaging on virtually every substrate up to frequencies in the sub-THz range.

A LOOK AT CURRENT APPLICATIONS

Additive manufacturing technologies (AMTs) such as inkjet and 3D printing have gained significant consideration in the past years especially in the field of nanotechnology and flexible electronics. AMTs are capable of producing flexible, conformal, and rollable devices by printing onto flexible substrates. In addition, introducing the third dimension allows the deposition of new nanotechnology-enabled materials with mechanical, topological, and physical properties unavailable in the realm of two-dimensional (2D) printing. The 3D- and inkjet-printing techniques offer a dramatically reduced setup cost, high repeatability, wide scalability, and environmental friendliness as compared to the traditional subtractive processes such as milling and lithography. AMTs involve a layer-by-layer deposition of different materials to form complex 3D objects without wasting much or any material [1], [2].

Among its numerous advantages, inkjet printing offers an easy realization of multilayer structures by sequentially depositing different types of inks to form each layer. This results from the fact that it is capable of the direct deposition of a wide range of materials such as conductive, dielectric, and semiconductor inks on a variety of substrates including paper, glass, semiconductor wafers, and polymers [3]–[5].

Additionally, 3D-printing technologies focus on the ability to print free-form 3D objects both with and without support materials, which cannot be produced by conventional subtractive manufacturing tools, such as interior cavities and meshes that allow the tuning of dielectric constant values. The typical feature size achieved using inkjet-printing technology and 3D-printing technology is 1–20 μm and 10–50 μm, respectively, making them very suitable for the realization of RF and mm-wave applications such as IoT motes, 5G systems, and smart skins (SS).

This article discusses the critical importance of nanotechnology to the additive manufacturing of a groundbreaking new generation of flexible microwave electronics and systems (whose typical structure is shown in Figure 1).

FABRICATION OF ULTRASENSITIVE FLEXIBLE AND ROBUST CHEMICAL SENSORS

Among commonly used flexible substrates, Kapton polyimide films possess particularly attractive mechanical and electrical properties as well as thermal and chemical stabilities. Their highly hydrophobic surface (with a water contact angle of 76° [6]) normally allows for the material deposition with hydrophobic fluids (solutions, suspensions, inkjet inks, and so on) but inhibits deposition with hydrophilic fluids. However, fabrication of an entire flexible electronic device often needs the deposition with both hydrophobic and hydrophilic fluids on the same substrate, which raises the need for surface modification of Kapton films to adjust their surface properties (particularly surface hydrophobicity) to facilitate the fabrication of flexible electronic devices.

Traditionally, polyimide films are surface modified with a number of approaches such as plasma [7], [8] and ion-beam [9], [10] etching, ultraviolet/ozone exposure [7], [11], acid [7], [12] and/or base [13], [14] treatments, and laser ablation [15], [16]. These traditional methods, which use harsh conditions, not only produce health-threatening and environmentally hazardous by-products or wastes but also compromise the structural integrity and the properties of the polyimide substrates. To alleviate these issues, several mild and environmentally friendly wet chemical approaches have been developed, which can minimize the compromise to the structural integrity and the properties of the substrates, to surface-modify Kapton polyimide films, thus efficiently tuning their surface properties. The resulting surface-modified Kapton films allowed for excellent printability of both hydrophobic and hydrophilic inkjet inks.

One of these novel surface modification approaches involved the use of two oppositely charged weak polyelectrolytes, polyethylenimine and poly(acrylic acid), to build, in a layer-by-layer fashion, a thin film of polyelectrolyte multilayers (PEMs) on Kapton HN films [6]. This work is the first demonstration of using only weak polyelectrolytes to efficiently surface-modify Kapton films. Compared to strong polyelectrolytes, weak electrolytes have the advantage of controlling the PEM properties more systematically and simply [17]. This work is also the first to make use of the surface properties of the additive particles embedded in the polyimide matrix.

As a conceptual demonstration of the general applications of this PEM-based surface modification approach, a flexible and robust gas sensor was fully inkjet printed on the resulting Kapton film with a homemade water-based graphene oxide (GO) nanoparticle ink and a commercial organic solvent-based silver nanoparticle (SNP) ink and assessed for its sensitivity to 2.0-ppm diethyl ethylphosphonate (DEEP), a G-series nerve agent simulant. The adhesion sustainability tests showed that the electrical conductivity and morphology of the sensor were insensitive to repeated bending around a 1-cm radius [6].

A second approach, which was inspired by the in vivo antagonizing interaction of heparin and protamine, used two environmentally friendly clinical biomolecules to deposit heparin-protamine complex on Kapton HN films in water-based salt solutions at neutral pH, room temperature, and atmospheric pressure [18]. This bioenabled approach is not only the first to utilize clinical biomolecules for substrate surface modification, but also the first surface modification approach performed under minimally destructive and maximally mild conditions.

After the surface modification, two types of reduced graphene oxide (rGO)-based flexible, ultralightweight, and miniature-sized gas sensors, with one

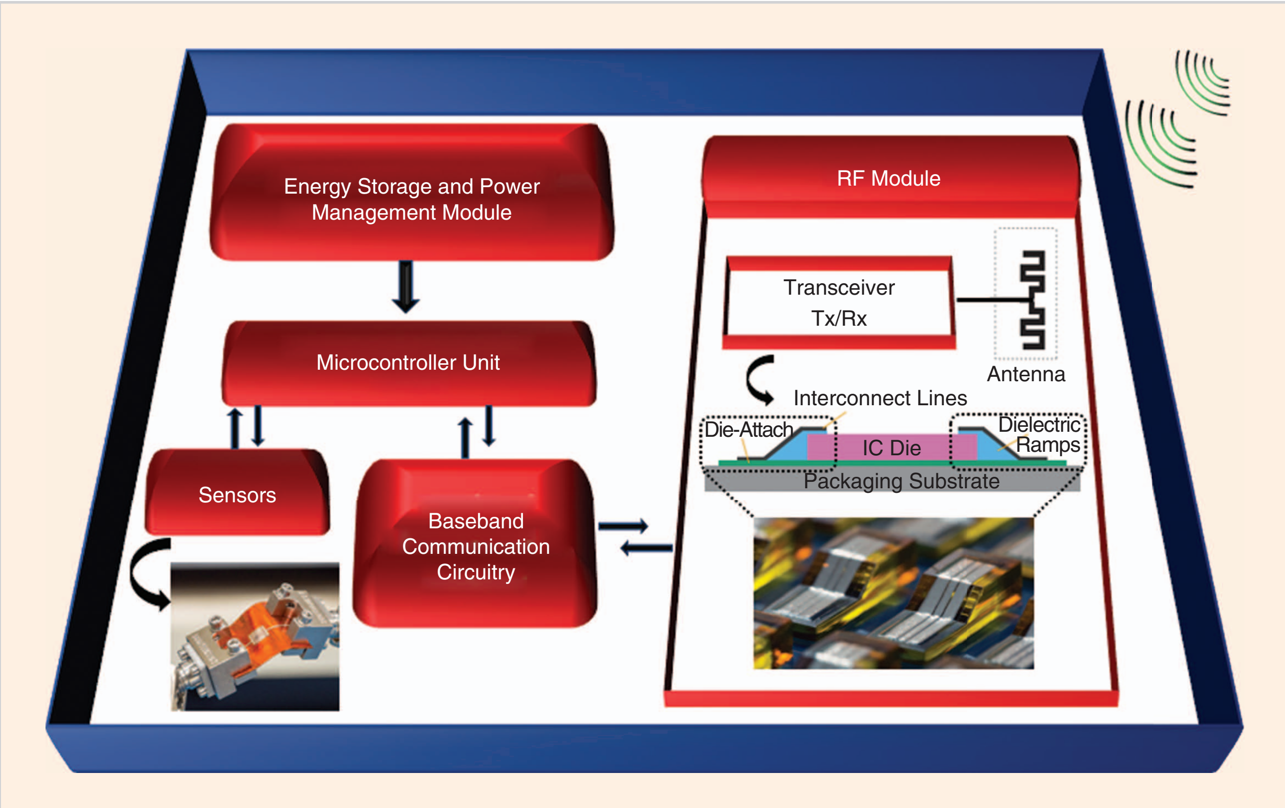

FIGURE 1 A system schematic of a typical IoT wireless sensor module.

functionalized with a chemoselective compound [2-(2-hydroxy-1, 1, 1, 3, 3, 3-hexafluoropropyl)-1-naphthol] and the other not, were inkjet printed with a homemade water-based GO nanoparticle ink and a commercial organic solvent-based SNP ink on the resulting Kapton films and tested for their sensitivity to dimethyl methylphosphonate (DMMP, a nerve agent simulant). The sensors survived a standard Scotch tape peel test and were shown to be insensitive to repeated bending to a small 0.5-cm radius.

Figure 2(a) shows an optical image of a flexible gas sensor that was inkjet printed on a piece of Kapton HN film that has been surface modified with this bioinspired approach. Figure 2(b) includes a scanning electron microscopy (SEM) image of an inkjet-printed silver interdigitated electrode (IDE) focused on the individual silver nanoparticles. Figure 2(c) shows an SEM image of the rGO film focused on the nanoscale rGO wrinkles. Figure 2(d) details the sensing behavior, upon exposure to 2.5-ppm DMMP vapor, of the sensors with (black solid line) and without (gray dashed line) the chemoselective compound 2-(2-hydroxy-1, 1, 1, 3, 3, 3-hexafluoropropyl)-1-naphthol.

To further enhance the sensitivity, novel approaches were developed that effectively modify the materials and the geometry of inkjet-printed IDEs, thus, drastically enhancing the sensitivity of the sensors. First, a novel layer-by-layer wet chemical approach was developed to uniformly deposit semiconducting single-walled CNTs (SWCNTs) on flexible Kapton films. Second, silver IDEs were inkjet-printed on the resulting SWCNT film. Finally, the dense silver IDEs were converted into their highly porous gold counterparts [19]. The following reaction was used to convert the dense silver IDEs into their dense Au-AgCl composite counterparts:

$$3Ag(s) + HAuCl_4(aq) \rightarrow Au(s) + 3AgCl(s) + HCl(aq). \quad (1)$$

Highly porous gold IDEs were obtained via selective dissolution of AgCl with a saturated aqueous NaCl solution. The porosity of the resulting highly porous gold IDEs was estimated to be as high as 67%. Figure 3(a) shows an array of such-fabricated flexible gas sensors, while Figure 3(b) reveals such a single sensor (at a higher magnification) with more morphological details. Figure 3(c) shows the nanoscale SWCNTs deposited on the Kapton film, while Figure 3(d) reveals the inkjet-printed dense silver IDEs focused on the individual silver nanoparticles.

After the conversion of the dense silver IDEs to their highly porous gold counterparts, the resulting gold IDEs were morphologically similar to the starting silver IDEs [Figure 3(b)] under low magnifications, but they were different in color. SEM analyses of the

To further enhance the sensitivity, novel approaches were developed that effectively modify the materials and the geometry of inkjet-printed IDEs, thus, drastically enhancing the sensitivity of the sensors.

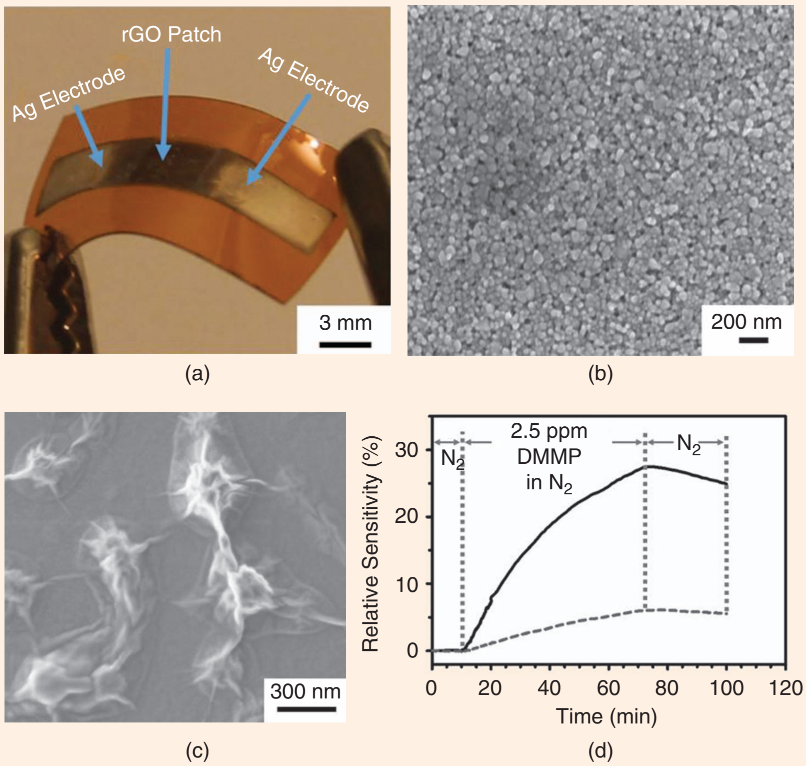

FIGURE 2 The characterization of an rGO-based flexible gas sensor that has been inkjet-printed on a Kapton HN film that was surface modified with the bioinspired approach. (a) An optical image of the sensor. (b) A high-magnification SEM image of a silver IDE of the sensor showing the individual silver nanoparticles. (c) A high-magnification SEM image of the rGO patch of the sensor focused on the nanoscale wrinkles of rGO. (d) The sensing behavior of the sensors with (black solid line) and without (gray dashed line) the chemoselective compound 2-(2-hydroxy-1, 1, 1, 3, 3, 3-hexafluoropropyl)-1-naphthol upon exposure to 2.5-ppm DMMP [18].

gold IDEs show their highly porous nature [Figure 3(e)]. Figure 3(f) shows the sensing behavior, upon exposure to 2.0-ppm DEEP vapor, of the sensors with dense silver IDEs (dash-dot line) and with porous gold IDEs (solid line), indicating that the conversion of the original inkjet-printed dense silver IDEs into their highly porous gold counterparts increased the sensor sensitivity by more than five times. This work suggested that the electrode material and/or the Schottky contacts between the electrodes and the semiconducting SWCNTs might have played an important role in the gas sensing process.

INKJET PRINTING OF FOLDABLE ELECTRICAL METAL TRACES ON CELLULOSE PAPER FOR ORIGAMI ELECTRONICS

One of the key limitations in the realization of low-cost complex multilayer flexible integrated sensors and communication systems for IoT applications is a reliable implementation of flexible conductive traces and interconnects. Although the cost can be significantly reduced by using low-cost organic substrates such as paper, most conductive inks are inflexible as they go through the sintering process and typically crack or break when bent or folded.

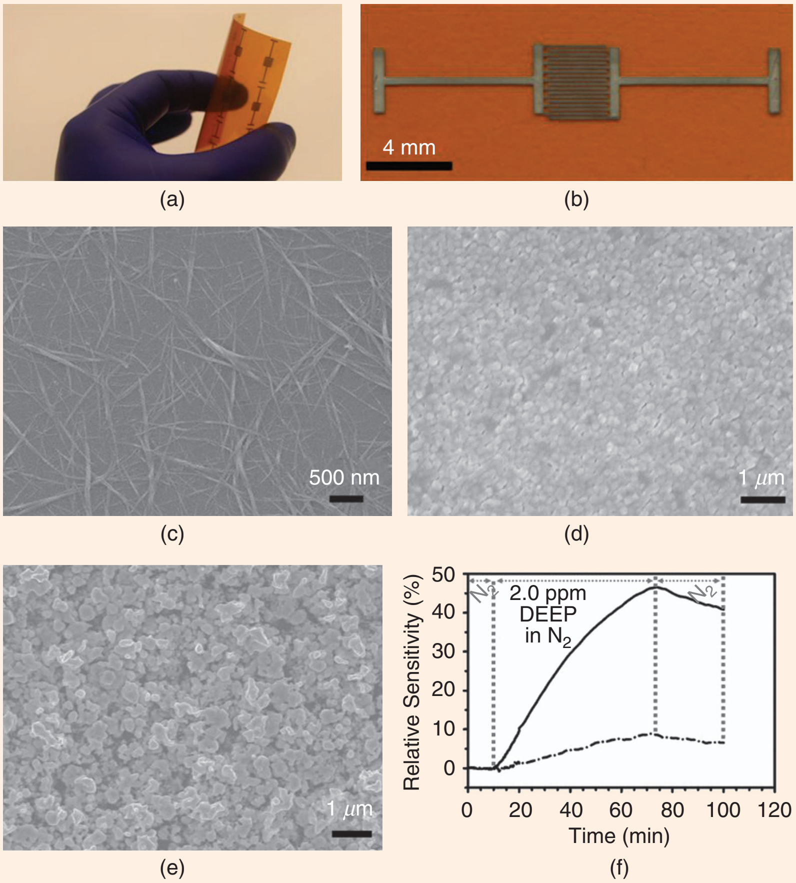

FIGURE 3 The characterization of semiconducting SWCNT-based flexible gas sensors fabricated on a Kapton HN film. (a) An optical image of an array of such sensors. (b) A scanned image of an inkjet-printed silver-electrode sensor. (c) A high-magnification SEM image of the SWCNT film of the sensor focused on the individual nanoscale SWCNTs. (d) A high-magnification SEM image of a silver IDE of the sensor showing the individual silver nanoparticles. (e) A high-magnification SEM image of a resulting highly porous gold IDE of the sensor showing the individual gold nanoparticles after the dense silver IDEs have been converted into their highly porous gold counterparts. (f) The sensing behavior of the proof-of-concept SWCNT-based sensors with dense silver IDEs (dash-dot line) and with porous gold IDEs (solid line) upon exposure to 2.0-ppm DEEP vapor [19].

This problem is even more pronounced in realization of via holes for multilayer structures that are typically achieved by drilling (conical-shaped) holes in the substrate then filling them with conductive epoxy [20] or using inkjet-printing conductive ink on via sidewalls [21] to create electrical contact with other substrates for multilayer structures [1], [22], [23]. However, these via geometries are complex to ensure better side-wall coverage for inkjet printing, similarly the conductive epoxies typically feature limited flexibility that cracks when bent. This section introduces a unique state-of-the-art methodology to realize through substrate drill-less via holes and flexible conductive traces that do not require physically etched vias and still maintains a very good electrical conductivity and RF performance when bent or folded.

INKJET-PRINTED DRILL-LESS VIAS ON PAPER

Interconnects are fundamental to realize the next generation of multilayer electrical and RF structures for IoT, SS, and 5G technologies. Vias provide an electrical pathway between intermediate layers. However, they can introduce significant parasitic inductance and capacitance that can affect the overall performance of the system. Moreover, the design is further complicated for flexible structures where the vias can crack under bending and create unwanted local reflections and standing waves. Therefore, efficient interconnect/via design is essential for high-performance RF circuits and components. Previously, a number of techniques were introduced to realize microvias that include laser [23] or chemical [22] etching for a fully inkjet-printed via with polymer-based ink with sidewalls that were inkjet printed with conductive ink for metallization to create an electrical short between the layers [24]. In [25], a stepped via approach was used to realize vias on relatively thick substrates with a diameter of 2 mm and conductivity of $7.4 \pm 2\Omega$.

A state-of-the-art technique to realize highly flexible fully inkjet-printed drill-less vias and through-substrate conductive traces was introduced in [26] that took advantage of high porosity of a normal (110-μm-thick) cellulose paper to absorb the solvent-based silver nanoparticle (SNP) ink, creating an electrical short across the thickness of the paper after curing. A cross-sectional view and surface profile of cellulose paper for a different number of layers of SNP ink is shown in Figure 4. It can be seen that SNP ink went through almost half the thickness of the cellulose paper when ten or more layers of SNP were inkjet-printed on one side of the substrate. Therefore, through-substrate conductivity (electrical short) can be realized by simply printing on both sides of the paper.

To evaluate the electrical and RF performance of these vias under bending, a fully inkjet-printed multilayer substrate-integrated waveguide (SIW) was fabricated on cellulose paper in [26] where the sidewalls of the SIW were electrically shorted by a through-substrate conductor wall as shown in Figure 5. It was shown in [26] that the performance of SIW did not change when bent from a flat configuration to a 10-mm radii of curvature. The high flexibility of the conductor traces as well as the through-substrate shorted conductor walls is mainly attributed to the fiber-like bulk structure of the printed silver within the paper, which tends to have the capability to accommodate for a large amount of stress without breaking.

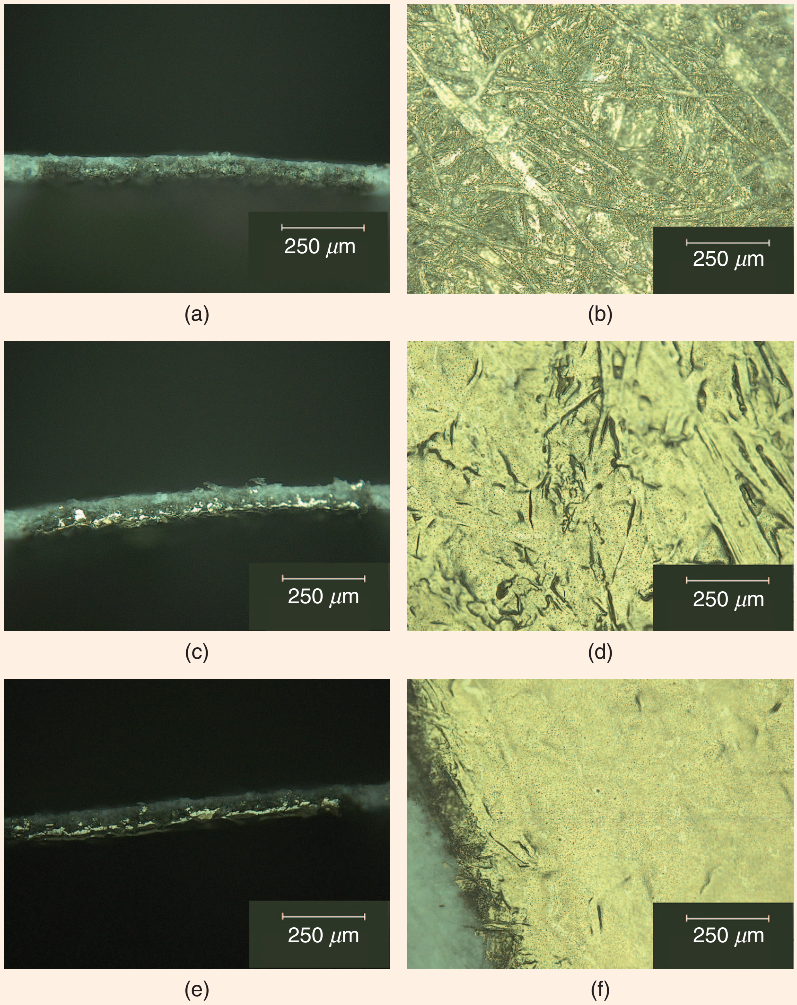

FIGURE 4 A cross-sectional view and surface profile of 1-mm-wide inkjet-printed lines with SNP ink for different number of layers [26]. (a) A one-layer cross-sectional view; (b) a one-layer surface profile; (c) a five-layer cross-sectional view; (d) a five-layer surface profile; (e) a 10-layer cross-sectional view; and (f) a 10-layer surface profile.

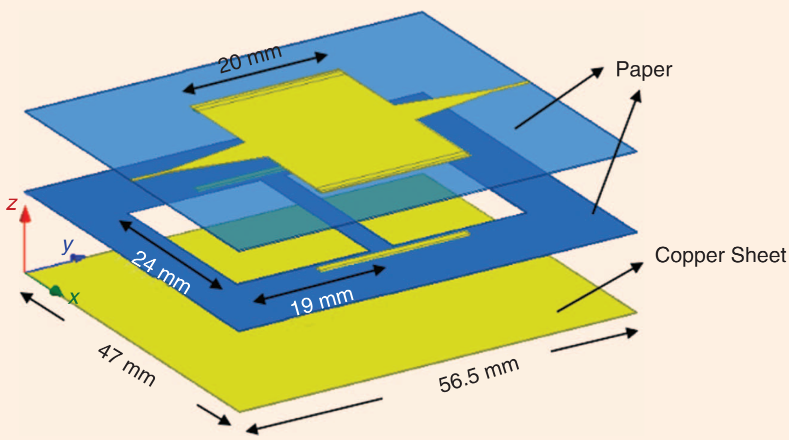

FIGURE 5 An exploded view of a fully inkjet-printed SIW [26].

SHAPE-SHIFTING TUNABLE RF STRUCTURES

The high flexibility of the conductive traces outlined in this section can be used to realize 4D shape-shifting, fully inkjet-printed RF structures that can tune their electrical, mechanical and RF behavior in response to change in their ambient conditions by simply changing the shape of the structure. This is in contrast to conventional techniques use varactors [27], [28], diodes [29]–[31], microelectromechanical systems, or change the electrical properties of the substrate [32] to tune the frequency response of the RF structures. However, these techniques feature limited tunability (15–20% frequency shift), expensive, laborious, and become unrealistic for large RF structures.

Some of the early examples of these 4D structures included an origami-inspired reconfigurable antenna that was realized using copper tape on cellulose paper and could change its resonance frequency by varying its height [33]. Such RF structures are lightweight, compact, and features high tunability, that is why they have found applications in many areas including aerospace [34], biomedicine [35], and deployable mechanical structures [36]. However, conventional fabrication technologies either use copper tape or custom-made substrates [37] that limit their usability in practical applications. Therefore, the fully inkjet-printed flexible conductive traces presented in this section presents an attractive alternative to realize such structures due to its low cost, simplicity, high repeatability, and good RF performance.

A novel 4D fully inkjet-printed tunable frequency selective surface (FSS) was realized in [2] and [38] using inkjet-printed dipole elements across the foldlines of a Miura-Ori (origami) structure on a cellulose paper as shown in Figure 6(a). Note that simple dipole elements were used in this case as a proof-of-concept demonstration of highly tunable RF structures that maintain good electrical and RF response even undergoing extreme bending and folding. Moreover, special bridge-like structures were employed along the dipole structures that allow the dipoles, as shown in Figure 6(c), to curve along the foldlines instead of forming a sharp bend as the Miura structure is folded, thereby further improving the flexibility of the conductive traces. The simulated and measured results show more than 15% tunability, which can be significantly improved by introducing more folds along the length of the dipole structures. Moreover, the response of the Miura FSS remains unchanged with respect to the angle of arrival of the incident wave.

INTERNET OF SKINS WIRELESS PRINTED FLEXIBLE SYSTEMS

The different nanomaterials innovations described previously, from the printed sensing elements to the substrate preparation techniques, and the nanomaterials-based inks have permitted the realization of novel systems whose features and form factors would have previously been technologically unattainable. One particularly fruitful area for such developments has been that of wireless SS, whose advent was triggered by the increasing availability of low-cost additive manufacturing tools for flexible and thin-circuit rapid design and fabrication.

From a wireless technology standpoint, such skins can be broadly classified into two distinct groups: chipless and nonchipless. This classification, while seemingly quite trite, has far-reaching consequences on the design considerations required for the implementation of given systems in either category, which we will cover and provide examples of in the sections “Chipless Skins” and “Semipassive Approach.”

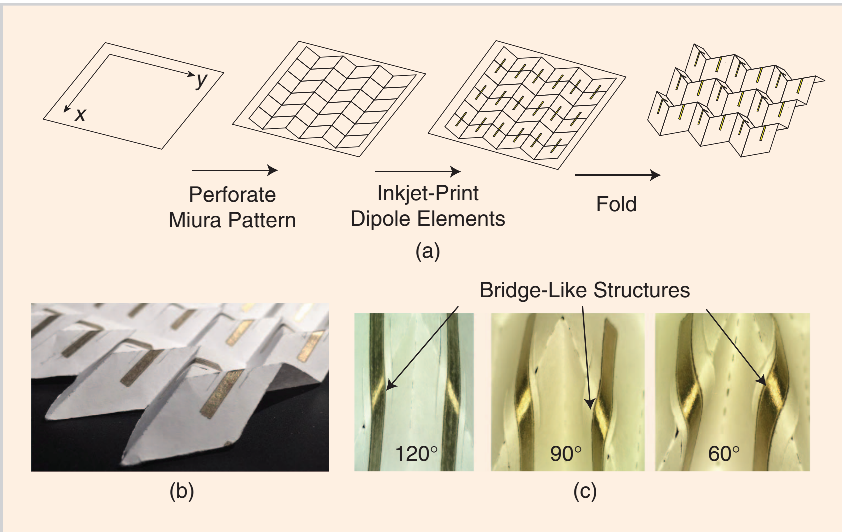

FIGURE 6 (a) The fabrication process for single-layer Miura FSS, (b) a close-up picture of fabricated design, and (c) micrograph of dipole elements with different folding angle θ.

CHIPLESS SKINS

In chipless skins, any information—whether structurally encoded such as an identification number, or environmentally modulated such as for a sensor—needs to be embedded and communicated at a single frequency of operation at a given instant. Such linear devices can therefore only be assembled from elements that provide a recognizable signature in the RF and mm-wave ranges.

With this in mind, proper characterizations of the high-frequency properties of the sensing material films described previously become essential. Such an effort, reported in [41], describes such analysis and the modeling of the fully inkjet-printed carbon-nanotubes-based breath sensor shown on Figure 7(c), in the 500-MHz to 2-GHz frequency range. The modeling approach uncovered an equivalent electrical model for the sensor, shown in Figure 7(d), whose intrinsic (solely associated with the CNT film and, therefore, variable upon sensing) and extrinsic components provided a very accurate matching of the S-parameters measured characterization data.

Chipless SS have also recently displayed significant improvements in their wireless communication capabilities with the introduction of flexible sticker-like reflectarray structures, such as the tag displayed in Figure 7(a). In recent efforts ([39], [40], [42], [43]), the identification, localization, and polling of such a fully printed humidity-sensing skin operating in the 30–40 GHz band was demonstrated at a range exceeding 50 m, representing more than an order of magnitude increase in the reading range of chipless tags.

SEMIPASSIVE APPROACH

While the previously reported recent progress of chipless skins is opening new and exciting application avenues for fully printed SS, these remain significantly less capable than their dc-powered nonlinear counterparts. Nevertheless, the unique nanomaterials-enabled abilities leveraged for the design and printing of chipless tags can similarly be strategically implemented into semipassive targets/sensors, such as the one shown in Figure 7(b). This flexible 28-GHz-operating printed system reported in [44] integrates an ultrahigh-sensitivity fully inkjet-printed, polyaminobenzene sulfonic acid-functionalized, CNT-based ammonia sensor, a fully printed backscatter-modulating reflectarray, and commercial integrated circuits and flexible amorphous-silicon solar cell. The tag, exploiting the same electromagnetics principles responsible for the unprecedented range of the chipless tag shown on Figure 7(a), demonstrated, at the time of its publication, the longest reported range for a backscatter device and an ability to sense and communicate the presence of ammonia in real time using only 200 μW of harvested indoor-lighting-sourced power.

THE 3D PRINTING OF FUNCTIONAL DEVICES

INKJET PRINTING OF PASSIVE ELECTRONICS

In the last decade, there has been rapid growth in 3D printing, with recent advances bringing additional functionality to previously mechanical structures, including the integration of 3D-printed electronics. The utilization of nanoparticles in this field is critical for several technologies, from traditional fused deposition modeling (FDM), stereolithography (SLA), 3D inkjet printing, and many more additive processes. Nanoparticles enable the deposition of functional materials through continually shrinking orifices, which enables increased resolutions for next-generation applications. Current aerosol jet, inkjet printing, and direct-write technologies have resolutions as low as 10–20 μm, and to realize functional and dispensable inks and pastes, there becomes a necessity of nanoparticle solutions.

Utilized in practically every circuit, passive resistor, inductor, and capacitor components are crucial for the progression of functional additive manufacturing, with high-performance devices being reliant on functional nanomaterials. Multilayer capacitors have been demonstrated utilizing a multilayer approach of SU-8 and poly(4-vinylphenol) and silver nanoparticle inks for utilization in the

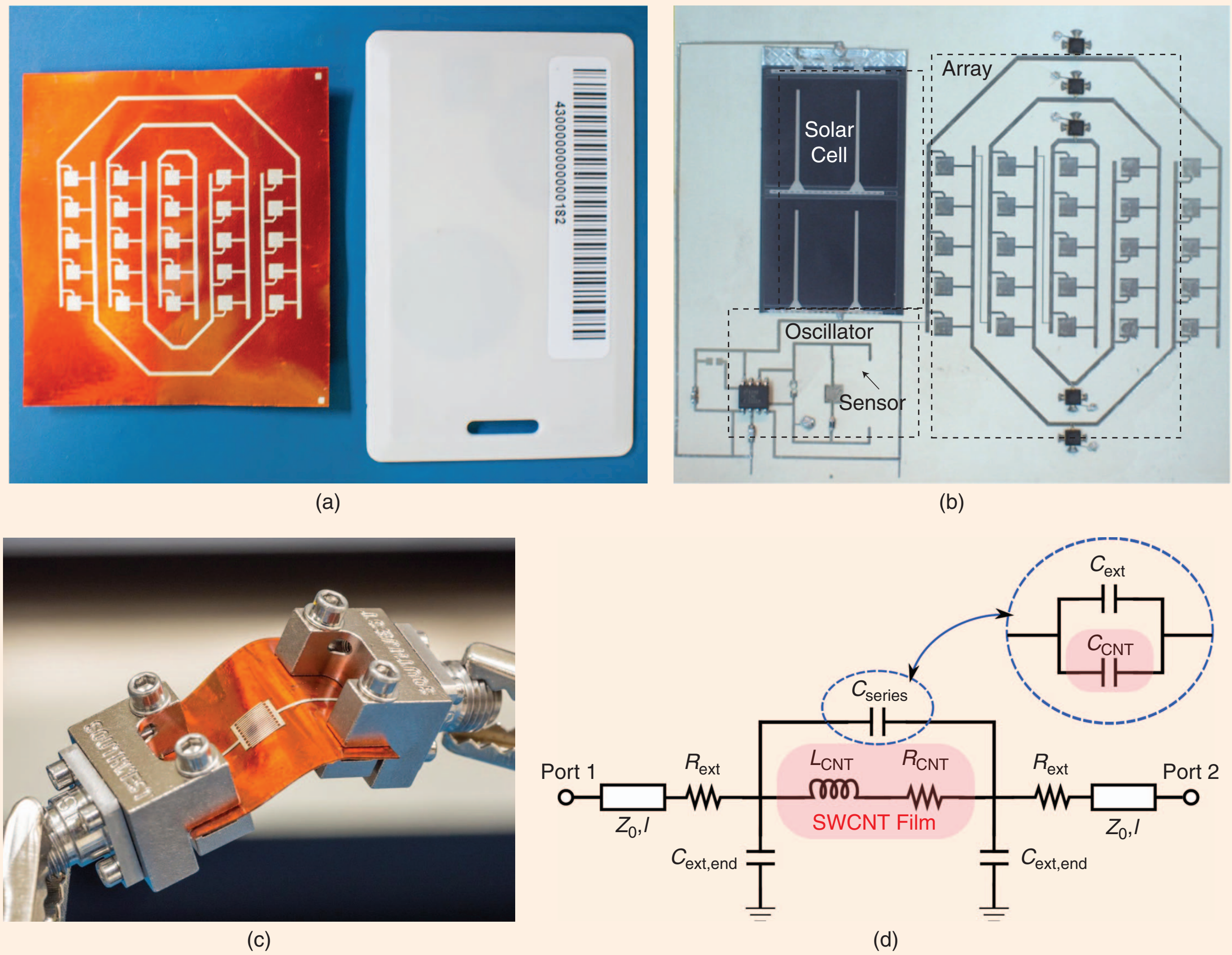

FIGURE 7 (a) An inkjet-printed flexible chipless humidity sensor prototype next to a standard credit card [39]. (b) A printed Van-Atta reflectarray wireless sensing system [40]. (c) A photo and (d) an equivalent model of a flexible, fully inkjet-printed SWCNT-based IDE breath sensor [41].

This article reviewed the recent nanotechnology-empowered advances in RF electronics achieved through additive manufacturing.

2.4 GHz industrial, scientific, and medical radio band [45]. Similarly, printed ferromagnetic inductors were realized with the use of a nanoparticle ferromagnetic ink. Utilizing cobalt nanoclusters that are coated with sodium dioctylsulfosuccinate to prevent conglomeration and oxidation [46]. The use of a 50-μm layer of the ferromagnetic ink demonstrates a size reduction of 12.5%, while maintaining a self-resonance frequency of 5 GHz. The expansion of utilizing inkjet printing for 3D printing enables the use of functional materials in complex, high-resolution, multimaterial 3D structures that is just beginning [47].

DIRECT WRITE OF FUNCTIONAL DEVICES FOR STRETCHABLE ELECTRONICS

The utilization of direct write technologies over aerosol jet or inkjet enables the deposition of higher-viscosity solutions between 1 cP to 1×10^6 cP, allowing for a wider range of compatibility with nanoparticle solutions. For example, electrically conductive adhesives (ECAs) utilizing silver flakes (Figure 8) enable constant high conductivity up to $1.51 \times 10^4 \mathrm{~S\,cm}^{-1}$ that remains constant within an order of magnitude with a strain of 240% [48]. The ability to strain and maintain conductivity is critical for next-generation stretchable electronics, and nanomaterial-based stretchable conductors enable high-performance reconfigurable antennas. By 3D printing the ECA silver flake material via direct write on an FDM-deposited thermoplastic polyurethane elastomer, a strain-sensitive object is demonstrated for 2.4-GHz applications [49]. Utilizing an nScrypt direct-write tool with the ECA, several resonators are printed onto a silicone substrate, each acting as a bandstop filter for chipless RF identification purposes. As each resonator changes shape or decouples from a transmission line due to deforming, the system response varies accordingly, and with each resonator correlated to the fingers on a hand, a chipless smart surface is fabricated to enable wireless and battery-less hand gesture sensing [50].

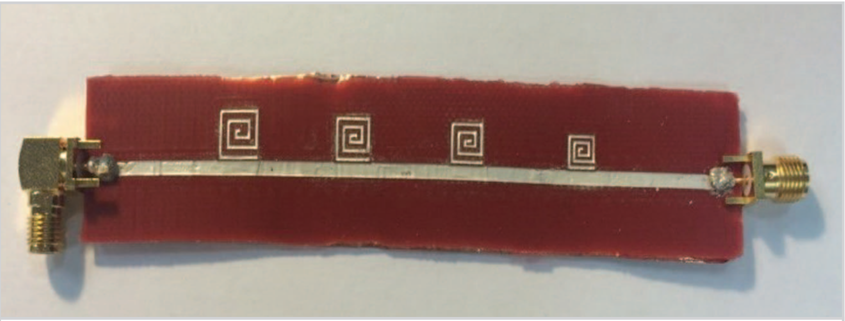
FIGURE 8 A direct-written hand gesture sensor using silver flakes [50].

ADDITIVE MANUFACTURING FOR HIGH-PERFORMANCE 3D RF INTERCONNECTS

The field of microelectronic packaging for wireless applications is currently focusing on several key technological developments: low-loss materials, low-loss interconnects, and efficient system-level integration. For decades, epoxy mold compounds (EMCs) featuring micron-scale silica and AlN particle loadings have been utilized for chip encapsulation, enabling the control of the dielectric constant, loss tangent, and coefficient of thermal expansion of the encapsulant [51], [52]. The inclusion of nanoparticles has also been investigated for the enhancement of EMC fracture toughness with thermal stress [53]. Interconnection between a wireless chip and a packaging substrate, such as a lead frame, is typically achieved through thermosonic wire-bonding techniques. These wire bond interconnects are inexpensive and used widely throughout industry, however passive compensation circuits are typically required to account for the high series inductance (approximately $1 \mathrm{~nH\,mm}^{-1}$) found in bond wires [54], [55].

The development of efficient interconnects plays directly into SiP design schemes, where active radios and passive components (antennas, bypass capacitors, matching networks, and others) are all integrated within a single package to reduce system losses and allow for device miniaturization. This section focuses on the development of low-loss and robust 3D RF interconnects using nanoparticle-based inks with additive inkjet-printing fabrication technology for mm-wave wireless SiP packaging.

INKJET-PRINTED 3D RAMP INTERCONNECTS WITH NANOPARTICLE-BASED CONDUCTIVE INK

Recent efforts in the development of low-loss RF interconnects have introduced additive inkjet-printing technology as a candidate for replacing standard wire-bonding techniques with wireless packages [56], [57]. As previously highlighted, silver nanoparticle-based inks allow for the patterning of conductive features on a wide variety of substrates in a low-temperature (<200 °C) fashion. This process eliminates the thermosonic bonding process used with wire bonding and, as a result, reduces the physical and thermal stresses placed on a die during the interconnection process.

A 2D side-view schematic of inkjet-printed 3D ramp interconnects is shown in Figure 9(a). First, an SU-8 photoresist-based dielectric ink is printed to pattern the 3D ramp structures bridging the top of the packaging substrate to the top plane of the die. Once the 3D ramps are patterned, a silver nanoparticle-based ink is printed to pattern coplanar waveguide (CPW) RF interconnects directly onto the printed ramps, providing a 50-Ω RF interconnect for a surface-mount die. Finally, thermal sintering takes place at 180 °C for 1 h in order to achieve conductive features while maintaining a low-temperature process. Figure 9(b)–(d) includes images of fully printed 3D ramp interconnects for integration with wireless devices on the die level. S-parameter measurements of these interconnects yield a line loss of $0.6-0.8\,\text{dB}\,\text{mm}^{-1}$ at 40 GHz along with an inductance of $0.4-0.5\,\text{nH}\,\text{mm}^{-1}$, approximately half of the inductance of a typical wire bond [54]. Integration with active Ka-band devices (26.5–40 GHz) is currently a focus in order to further evaluate the effectiveness of nanoparticle-based inkjet printing for mm-wave wireless packaging [58].

We demonstrated the realization of 4D fully inkjet-printed reconfigurable frequency RF architectures based on shape tunability, which opens a new opportunity in the area of reconfigurable RF structures.

FULLY PRINTED THROUGH-MOLD VIAS FOR APPLICATION-SPECIFIC WIRELESS PACKAGING

The efforts presented in the "Inkjet-Printed 3D Ramp Interconnects With Nanoparticle-Based Conductive Ink" section demonstrate the effectiveness of inkjet printing silver nanoparticle-based and polymer-based inks to realize 3D RF interconnects from a substrate to a die. However, truly 3D integration is still lacking.

To realize high-aspect-ratio 3D RF interconnects, inkjet printing can be combined with SLA 3D printing in a purely additive fashion. The combination of these technologies allows for the development of smart die encapsulants with embedded vias, or through-mold vias (TMVs), to interface with subsequently printed topologies above an encapsulated die [57]. Figure 10(a)–(d) presents process-flow schematics for the development of printed TMVs within die encapsulants [59].

The use of silver nanoparticle-based inks with inkjet printing is critical to the realization of these embedded via structures due to the low-temperature processes and conformal nature of inkjet printing combined with 3D printing. The effects of printing conformally onto 3D slopes is investigated in [57], where it is determined that printed interconnects can be achieved with slopes up to 65°.

Figure 10(e) shows a perspective image of a TMV test vehicle with 35° slope TMVs fabricated with 3D SLA-printed photopolymer ramp structures and inkjet-printed silver nanoparticle RF CPW interconnects. The interconnects presented in this effort yield a line loss of less than $0.5-0.6\,\text{dB}\,\text{mm}^{-1}$ up to 60 GHz, demonstrating a fully printed

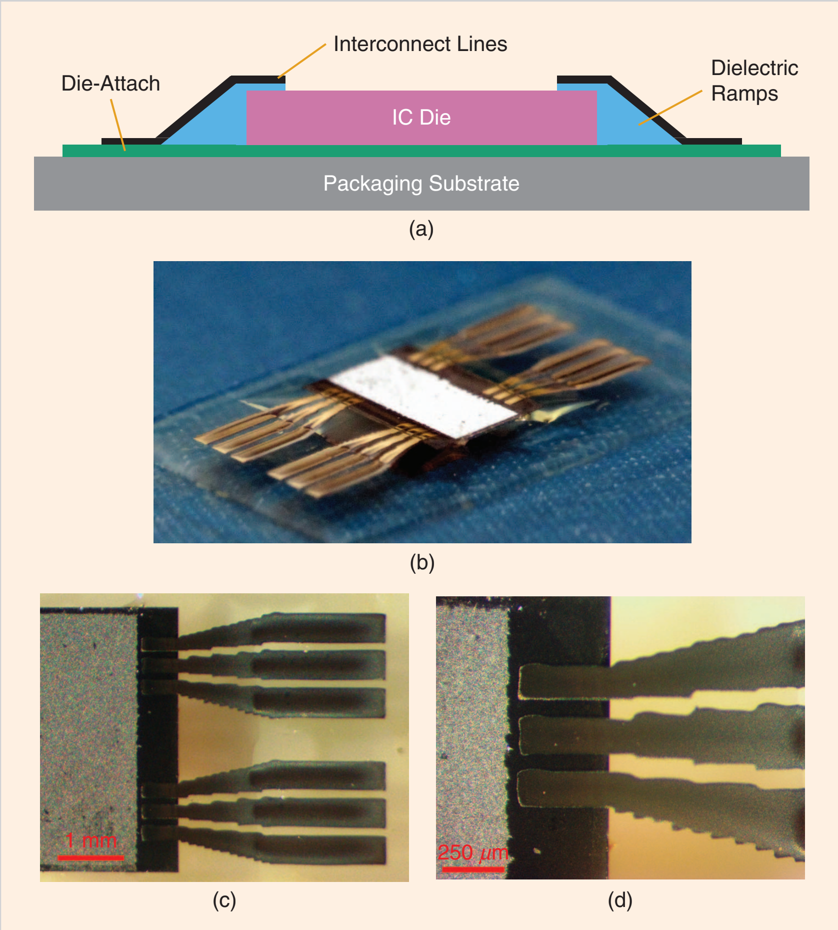

FIGURE 9 An inkjet-printed 3D RF interconnects with silver nanoparticle ink. (a) A cross-section schematic of printed RF interconnects; (b) a perspective image of the inkjet-printed CPW interconnect samples; and (c) and (d) detail micrographs [56]. IC: integrated circuit.

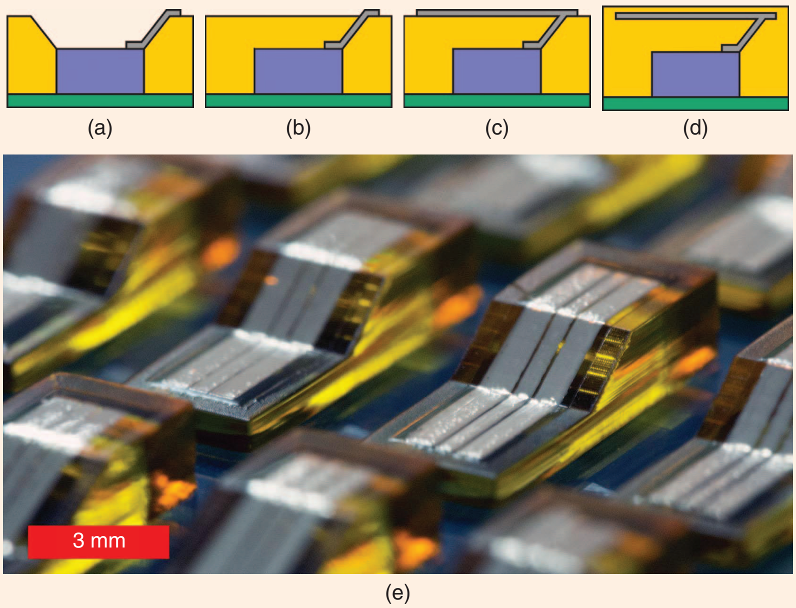

FIGURE 10 The smart wireless encapsulant process flow [59]. (a) A 3D print partial encapsulant with die and inkjet-print-sloped TMV using silver nanoparticle-based ink. (b) A cap partial encapsulant with photopolymer resin leaving an exposed TMV interconnecting to the embedded die. (c) An inkjet-printed antenna, passive, or other SiP component. (d) The 3D-printed final encapsulant. (e) Fully inkjet/3D-printed TMVs using silver nanoparticle-based ink [57].

low-loss RF interconnect for integration with wireless SiP design schemes, enabled through the utilization of conductive nanoparticle-based inks.

CONCLUSION

This article reviewed the recent nanotechnology-empowered advances in RF electronics achieved through additive manufacturing. The presented printed structures prove the potential applications provided by the AMTs involving a variety of the nanomaterial-based inks on a diverse choice of substrates.

We demonstrated the realization of 4D fully inkjet-printed reconfigurable frequency RF architectures based on shape tunability, which opens a new opportunity in the area of reconfigurable RF structures. In addition, we highlighted the role of nanoparticles-based inks in the birth of low-cost and power-autonomous printed motes for the IoT and mm-wave 5G cellular networks.

As we have shown, this rise in maturity has provided a new framework within which the RF research community has been able to imagine and demonstrate entirely printed passive electronics with the integration of 3D-printed RF interconnects. In addition, taking full advantage of the presented additive manufacturing approaches would be by developing reliable and scalable manufacturing means with repeatability and process variations comparable to existing approaches.

ACKNOWLEDGMENT

We would like to thank the National Science Foundation, Semiconductor Research Corporation, and the Defense Threat Reduction Agency for their support during this project.

ABOUT THE AUTHORS

Aline Eid (aeid7@gatech.edu) is with the School of Electrical and Computer Engineering, the Georgia Institute of Technology, Atlanta.

Jimmy Hester (jimmy.hester@gatech.edu) is with the School of Electrical and Computer Engineering, the Georgia Institute of Technology, Atlanta.

Yunnan Fang (yfang6@mail.gatech.edu) is with the School of Materials Science and Engineering, Georgia Institute of Technology, Atlanta.

Bijan Tehrani (btehrani3@gatech.edu) is with the School of Electrical and Computer Engineering, the Georgia Institute of Technology, Atlanta.

Syed Abdullah Nauroze (nauroze@gatech.edu) is with the School of Electrical and Computer Engineering, the Georgia Institute of Technology, Atlanta.

Ryan Bahr (rbahr@gatech.edu) is with the School of Electrical and Computer Engineering, the Georgia Institute of Technology, Atlanta.

Manos M. Tentzeris (etentze@ece.gatech.edu) is with the School of Electrical and Computer Engineering, the Georgia Institute of Technology, Atlanta.

REFERENCES

[1] S. A. Nauroze, J. G. Hester, B. K. Tehrani, W. Su, J. Bito, R. Bahr, J. Kimionis, and M. M. Tentzeris, “Additively manufactured rf components and modules: Toward empowering the birth of cost-efficient dense and ubiquitous IoT implementations,” *Proc. IEEE*, vol. 105, no. 4, pp. 702–722, 2017.

[2] J. G. Hester, S. Kim, J. Bito, T. Le, J. Kimionis, D. Revier, C. Saintsing, W. Su, B. Tehrani, A. Traille, B. S. Cook, and M. M. Tentzeris, “Additively manufactured nanotechnology and origami-enabled flexible microwave electronics,” *Proc. IEEE*, vol. 103, no. 4, pp. 583–606, 2015.

[3] L. Yang, A. Rida, and M. M. Tentzeris, “Design and development of radio frequency identification (RFID) and RFID-enabled sensors on flexible low cost substrates,” *Synthesis Lectures RF/Microwaves*, vol. 1, no. 1, pp. 1–89, 2009.

[4] S. H. Ko, J. Chung, H. Pan, C. P. Grigoropoulos, and D. Poulikakos, “Fabrication of multilayer passive and active electric components on polymer using inkjet printing and low temperature laser processing,” *Sensors Actuators A: Physical*, vol. 134, no. 1, pp. 161–168, 2007.

[5] B. S. Cook, B. Tehrani, J. R. Cooper, and M. M. Tentzeris, “Multilayer inkjet printing of millimeter-wave proximity-fed patch arrays on flexible substrates,” *IEEE Antennas Wireless Propag. Lett.*, vol. 12, pp. 1351–1354, Oct. 2013.

[6] Y. Fang, J. G. Hester, B. M. deGlee, C.-C. Tuan, P. D. Brooke, T. Le, C-p Wong, M. M. Tentzeris, and K. H. Sandhage, “A novel, facile, layer-by-layer substrate surface modification for the fabrication of all-inkjet-printed flexible electronic devices on Kapton,” *J. Mater. Chem. C*, vol. 4, no. 29, pp. 7052–7060, 2016.

[7] I. Gouzman, O. Girshevitz, E. Grossman, N. Eliaz, and C. N. Sukenik, “Thin film oxide barrier layers: Protection of Kapton from space environment by liquid phase deposition of titanium oxide,” *ACS Appl. Mater. Interfaces*, vol. 2, no. 7, pp. 1835–1843, 2010.

[8] N. Inagaki, S. Tasaka, and K. Hibi, “Surface modification of Kapton film by plasma treatments,” *J. Polym. Sci. A, Polym. Chem.*, vol. 30, no. 7, pp. 1425–1431, 1992.

[9] B. J. Bachman and M. J. Vasile, “Ion bombardment of polyimide films,” *J. Vacuum Sci. Technol. A: Vacuum, Surfaces, Films*, vol. 7, no. 4, pp. 2709–2716, 1989.

[10] J.-W. Shin, J.-P. Jeun, and P.-H. Kang, “Surface modification and characterization of n+ ion implantation on polyimide film,” *Macromolecular Res.*, vol. 18, no. 3, pp. 227–232, 2010.

[11] T. Le, V. Lakafosis, Z. Lin, C. Wong, and M. Tentzeris, “Inkjet-printed graphene-based wireless

gas sensor modules," in *Proc. 2012 IEEE 62nd Electronic Components and Technology Conf. (ECTC)*, 2012, pp. 1003–1008.
[12] I. Ghosh, J. Konar, and A. K. Bhowmick, "Surface properties of chemically modified polyimide films," *J. Adhesion Sci. Technol.*, vol. 11, no. 6, pp. 877–893, 1997.
[13] X. D. Huang, S. M. Bhangale, P. M. Moran, N. L. Yakovlev, and J. Pan, "Surface modification studies of Kapton® hn polyimide films," *Polymer Int.*, vol. 52, no. 7, pp. 1064–1069, 2003.
[14] R. R. Thomas, S. L. Buchwalter, L. P. Buchwalter, and T. H. Chao, "Organic chemistry on a polyimide surface," *Macromolecules*, vol. 25, no. 18, pp. 4559–4568, 1992.
[15] B. T. Least and D. A. Willis, "Modification of polyimide wetting properties by laser ablated conical microstructures," *Appl. Surf. Sci.*, vol. 273, pp. 1–11, May 2013.
[16] L. Gallais, E. Bergeret, B. Wang, M. Guérin, and E. Bènevent, "Ultrafast laser ablation of metal films on flexible substrates," *Appl. Phys. A*, vol. 115, no. 1, pp. 177–188, 2014.
[17] D. Yoo, S. S. Shiratori, and M. F. Rubner, "Controlling bilayer composition and surface wettability of sequentially adsorbed multilayers of weak polyelectrolytes," *Macromolecules*, vol. 31, no. 13, pp. 4309–4318, 1998.
[18] Y. Fang, J. G. Hester, W. Su, J. H. Chow, S. K. Sitaraman, and M. M. Tentzeris, "A bio-enabled maximally mild layer-by-layer Kapton surface modification approach for the fabrication of all-inkjet-printed flexible electronic devices," *Sci. Rep.*, vol. 6, pp. 39909, Dec. 2016.
[19] Y. Fang, M. Akbari, L. Sydänheimo, L. Ukkonen, and M. M. Tentzeris, "Sensitivity enhancement of flexible gas sensors via conversion of inkjet-printed silver electrodes into porous gold counterparts," *Sci. Rep.*, vol. 7, no. 1, pp. 8988, 2017.
[20] R. Moro, M. Bozzi, S. Kim, and M. Tentzeris, "Novel inkjet-printed substrate integrated waveguide (SIW) structures on low-cost materials for wearable applications," in *2012 42nd European Microwave Conf. (EuMC)*, Oct. 2012, pp. 72–75.
[21] S. Kim, H. Aubert, and M. M. Tentzeris, "An inkjet-printed flexible broadband coupler in substrate integrated waveguide (SIW) technology for sensing, RFID and communication applications," in *Proc. 2014 IEEE MTT-S Int. Microwave Symp. (IMS)*, 2014, pp. 1–4.
[22] T. Kawase, H. Sirringhaus, R. H. Friend, and T. Shimoda, "Inkjet printed via-hole interconnections and resistors for all-polymer transistor circuits," *Adv. Mater.*, vol. 13, no. 21, pp. 1601, 2001.
[23] T. Falat, J. Felba, A. Moscicki, and J. Borecki, "Nano-silver inkjet printed interconnections through the microvias for flexible electronics," in *Proc. 2011 IEEE 11th Conf. Nanotechnology (IEEE-NANO)*, 2011, pp. 473–477.
[24] G. McKerricher, J. Gonzalez, and A. Shamim, "All inkjet printed 3D microwave capacitors and inductors with vias," in *Proc. 2013 IEEE MTT-S Int. Microwave Symp. Dig.*, 2013, pp. 1–3.
[25] S. Kim, A. Shamim, A. Georgiadis, H. Aubert, and M. M. Tentzeris, "Fabrication of fully inkjet-printed vias and siw structures on thick polymer substrates," *IEEE Trans. Compon. Packag. Manuf. Technol.*, vol. 6, no. 3, pp. 486–496, 2016.
[26] S. A. Nauroze, J. Hester, W. Su, and M. M. Tentzeris, "Inkjet-printed substrate integrated waveguides (SIW) with "drill-less" vias on paper substrates," in *Proc. 2016 IEEE MTT-S Int. Microwave Symp. (IMS)*, 2016, pp. 1–4.
[27] C. Mias, "Varactor-tunable frequency selective surface with resistive-lumped-element biasing grids," *IEEE Microw. Compon. Lett.*, vol. 15, no. 9, pp. 570–572, 2005.
[28] B. Schoenlinner, A. Abbaspour-Tamijani, L. C. Kempel, and G. M. Rebeiz, "Switchable low-loss RF MEMS ka-band frequency-selective surface," *IEEE Trans. Microw. Theory Techn.*, vol. 52, no. 11, pp. 2474–2481, 2004.
[29] M. Li, B. Yu, and N. Behdad, "Liquid-tunable frequency selective surfaces," *IEEE Microw. Compon. Lett.*, vol. 20, no. 8, pp. 423–425, 2010.
[30] A. deC. Lima, E. A. Parker, and R. J. Langley, "Tunable frequency selective surface using liquid substrates," *Electron. Lett.*, vol. 30, no. 4, pp. 281–282, 1994.
[31] J. A. Bossard, X. Liang, L. Li, S. Yun, D. H. Werner, B. Weiner, T. S. Mayer, P. F. Cristman, A. Diaz, and I. Khoo, "Tunable frequency selective surfaces and negative-zero-positive index metamaterials based on liquid crystals," *IEEE Trans. Antennas Propag.*, vol. 56, no. 5, pp. 1308–1320, 2008.
[32] T. Chang, R. J. Langley, and E. A. Parker, "Frequency selective surfaces on biased ferrite substrates," *Electron. Lett.*, vol. 30, no. 15, pp. 1193–1194, 1994.
[33] X. Liu, S. Yao, S. V. Georgakopoulos, B. S. Cook, and M. M. Tentzeris, "Reconfigurable helical antenna based on an origami structure for wireless communication system," in *Proc. 2014 IEEE MTT-S Int. Microwave Symp. (IMS2014)*, 2014, pp. 1–4.
[34] W. D. Reynolds, S. K. Jeon, J. A. Banik, and T. W. Murphey, "Advanced folding approaches for deployable spacecraft payloads," in *ASME 2013 Int. Design Engineering Technical Conferences and Computers and Information in Engineering Conf.*, 2013, pp. V06BT07A043–V06BT07A043.
[35] K. Kuribayashi, K. Tsuchiya, Z. You, D. Tomus, M. Umemoto, T. Ito, and M. Sasaki, "Self-deployable origami stent grafts as a biomedical application of ni-rich tini shape memory alloy foil," *Mater. Sci. Eng.: A*, vol. 419, no. 1, pp. 131–137, 2006.
[36] A. Thrall and C. Quaglia, "Accordion shelters: A historical review of origami-like deployable shelters developed by the us military," *Eng. Structures*, vol. 59, pp. 686–692, 2014.
[37] M. Nogi, N. Komoda, K. Otsuka, and K. Suganuma, "Foldable nanopaper antennas for origami electronics," *Nanoscale*, vol. 5, no. 10, pp. 4395–4399, 2013.
[38] S. A. Nauroze, L. Novelino, M. M. Tentzeris, and G. H. Paulino, "Inkjet-printed '4D' tunable spatial filters using on-demand foldable surfaces," in *Proc. 2017 IEEE MTT-S Int. Microwave Symp. (IMS)*, June 2017, pp. 1575–1578.
[39] J. G. Hester and M. M. Tentzeris, "Inkjet-printed van-atta reflectarray sensors: A new paradigm for long-range chipless low cost ubiquitous smart skin sensors of the internet of things," in *Proc. 2016 IEEE MTT-S Int. Microwave Symp.*, 2016, pp. 1–4.
[40] J. G. D. Hester and M. M. Tentzeris, "Inkjet-printed flexible mm-wave Van-Atta reflectarrays: A solution for ultra-long-range dense multi-tag and multi-sensing chipless RFID implementations for IoT Smart Skins," *IEEE Trans. Microw. Theory Techn.*, vol. 57, no. 5, pp. 1303–1309, May 2017.
[41] J. G. Hester, M. M. Tentzeris, and Y. Fang, "UHF lumped element model of a fully inkjet-printed single-wall-carbon-nanotube-based inter-digitated electrodes breath sensor," in *Proc. IEEE 2016 Antennas and Propagation Society Int. Symp. (APSURSI)*, 2016, pp. 1959–1960.
[42] D. Henry, J. G. D. Hester, H. Aubert, P. Pons, and M. M. Tentzeris, "Long range wireless interrogation of passive humidity sensors using van-atta cross-polarization effect and 3D beam scanning analysis," in *Proc. 2017 IEEE MTT-S Int. Microwave Symp. (IMS)*, June 2017, pp. 816–819.
[43] D. Henry, J. G. D. Hester, H. Aubert, P. Pons, and M. M. Tentzeris, "Long-range wireless interrogation of passive humidity sensors using van-atta cross-polarization effect and different beam scanning techniques," *IEEE Trans. Microw. Theory Techn.*, vol. 65, no. 12, pp. 5345–5354, Dec. 2017.
[44] J. G. D. Hester and M. M. Tentzeris, "A mm-wave ultra-long-range energy-autonomous printed RFID-enabled Van-Atta wireless sensor: At the crossroads of 5G and IoT," in *Proc. 2017 IEEE MTT-S Int. Microwave Symp. (IMS)*, June 2017, pp. 1557–1560.
[45] B. S. Cook, J. R. Cooper, and M. M. Tentzeris, "Multi-layer RF capacitors on flexible substrates utilizing inkjet printed dielectric polymers," *IEEE Microw. Compon. Lett.*, vol. 23, no. 7, pp. 353–355, July 2013.
[46] H. Lee, M. M. Tentzeris, P. Markondeya, M. K. P. Raj, and Y. Kawahara, "Inkjet-printed ferromagnetic nanoparticles for miniaturization of flexible printed RF inductors," in *Proc. 2013 IEEE Antennas and Propagation Society Int. Symp. (APSURSI)*, July 2013, pp. 994–995.
[47] E. Saleh, F. Zhang, Y. He, J. Vaithilingam, J. L. Fernandez, R. Wildman, I. Ashcroft, R. Hague, P. Dickens, and C. Tuck, "3D inkjet printing of electronics using UV conversion," *Adv. Mater. Technol.*, vol. 2, no. 10, pp. 1700134.
[48] Z. Li, T. Le, Z. Wu, Y. Yao, L. Li, M. Tentzeris, K. Moon, and C. P. Wong, "Rational design of a printable, highly conductive siliconebased electrically conductive adhesive for stretchable radiofrequency antennas," *Adv. Functional Mater.*, vol. 25, no. 3, pp. 464–470, 2014.
[49] T. Le, B. Song, Q. Liu, R. A. Bahr, S. Moscato, C. P. Wong, and M. M. Tentzeris, "A novel strain sensor based on 3D printing technology and 3D antenna design," in *Proc. 2015 IEEE 65th Electronic Components and Technology Conf. (ECTC)*, May 2015, pp. 981–986.
[50] T. Le, R. A. Bahr, M. M. Tentzeris, B. Song, and C. P. Wong, "A novel chipless RFID-based stretchable and wearable hand gesture sensor," in *2015 European Microwave Conf. (EuMC)*, Sept. 2015, pp. 371–374.
[51] P. Gonon, A. Sylvestre, J. Teysseyre, and C. Prior, "Dielectric properties of epoxy/silica composites used for microlectronic packaging, and their dependence on post-curing," *J. Mater. Sci.: Mater. Electron.*, vol. 12, no. 2, pp. 81–86, Feb. 2001.
[52] J.-W. Bae, W. Kim, S.-H. Cho, and S.-H. Lee, "The properties of AlN-filled epoxy molding compounds by the effects of filler size distribution," *J. Mater. Sci.*, vol. 35, no. 23, pp. 5907–5913, Dec. 2000.
[53] J. T. Han and K. Cho, "Nanoparticle-induced enhancement in fracture toughness of highly loaded epoxy composites over a wide temperature range," *J. Mater. Sci.*, vol. 41, no. 13, pp. 4239–4245, July 2006.
[54] U. R. Pfeiffer, J. Grzyb, D. Liu, B. Gaucher, T. Beukema, B. A. Floyd, and S. K. Reynolds, "A chip-scale packaging technology for 60-ghz wireless chipsets," *IEEE Trans. Microw. Theory Techn.*, vol. 54, no. 8, pp. 3387–3397, Aug. 2006.
[55] Y. P. Zhang and D. Liu, "Antenna-on-chip and antenna-in-package solutions to highly integrated millimeter-wave devices for wireless communications," *IEEE Trans. Antennas Propag.*, vol. 57, no. 10, pp. 2830–2841, Oct 2009.
[56] B. K. Tehrani, B. S. Cook, and M. M. Tentzeris, "Inkjet-printed 3D interconnects for millimeter-wave system-on-package solutions," in *Proc. 2016 IEEE MTT-S Int. Microwave Symp. (IMS)*, May 2016, pp. 1–4.
[57] B. K. Tehrani, R. A. Bahr, W. Su, B. S. Cook, and M. M. Tentzeris, "E-band characterization of 3D-printed dielectrics for fully printed millimeter-wave wireless system packaging," in *Proc. 2017 IEEE MTT-S Int. Microwave Symp. (IMS)*, June 2017, pp. 1756–1759.
[58] B. K. Tehrani and M. M. Tentzeris, "Fully inkjet-printed ramp interconnects for wireless ka-band mmic devices and multi-chip module packaging," in *2018 European Microwave Conf. (EuMC)*, 2018, under review.
[59] B. Tehrani, R. Bahr, D. Revier, B. Cook, and M. Tentzeris, "The principles of 'smart' encapsulation: Using additive printing technology for the realization of intelligent application-specific packages for iot, 5g, and automotive radar applications," in *Proc. 2018 IEEE 68th Electronic Components and Technology Conf. (ECTC)*, 2018.